Journal of Orthopaedic Surgery and Research

RESEARCH

Open Access

A novel rat model of lumbar disc herniation induced by puncture: accurate positioning and controllable degree of herniation

Ming Yang[1†], Jiangling Zhou[1†], Qiandong Yang[1], Bo Yu[1], Juan Cai[1] and Tianyong Hou[1*]

Abstract

Background Lumbar disc herniation (LDH) is the serious stage of intervertebral disc degeneration (IDD), and the location and degree of intervertebral disc herniation are closely related to clinical symptoms and signs. However, there is currently no low-cost, high-benefit animal model to support in vivo research on LDH.

Method Expose the rat's lumbar 5/6 intervertebral disc through the space between the psoas major and erector spine muscles, and then use different lengths of puncture needles to control the degree of herniation and different puncture angles to push the nucleus pulposus tissue backwards to the different position. Observe the protrusion of intervertebral discs through MRI. Von Frey mechanical pain test and BBB score were used to evaluate the behavior of LDH rats. H&E and SF staining were used to observe the morphological changes after intervertebral disc herniation. Immunofluorescence was used to analyze the expression of Aggrecan (ACAN), IL-1β, TNF-α, and CD31 in intervertebral disc tissue.

Results LDH rat exhibit varying degrees of motor and sensory dysfunction. The nucleus pulposus tissue in the center of the intervertebral disc undergoes degenerative changes, with a decrease in the content of nucleus pulposus cells and proteoglycans, an increase in the expression of inflammatory factors in the protruding tissue, and neovascularization.

Conclusion We have successfully constructed rat models of different types of intervertebral disc herniation, including disc degeneration, bulging, central herniation, and lateral herniation, using the method of puncture of intervertebral discs. This animal model is consistent with the characteristics of LDH in terms of behavior, imaging, and histopathology.

Keywords Lumbar disc herniation, Intervertebral disc degeneration, Rat model, Puncture, Central herniation, Paramedian herniation

†Ming Yang and Jiangling Zhou contributed equally to this work.

*Correspondence:
Tianyong Hou
tianyonghou@tmmu.edu.cn
[1]Department of Orthopaedics, Southwest Hospital, Army Medical University (Third Military Medical University), Chongqing 400038, China

Introduction

Lumbar disc herniation (LDH) is a degenerative disease of the spine, which is mainly characterized by pain in the waist and radiation numbness and pain in the lower limbs [1]. It has a high incidence rate and high disability rate, which has caused a huge burden to patients and society [2]. LDH is caused by intervertebral disc degeneration (IDD) due to various reasons, resulting in the protrusion of the nucleus pulposus tissue from the ruptured annulus fibrosus and compression of the spinal cord or nerve roots. The outer layer of the intervertebral disc is a fibrous ring composed of many layers of collagen fibers arranged in concentric circles, while the inner layer is a high-water content and proteoglycan rich nucleus pulposus tissue [3]. This structure endows the intervertebral disc with excellent mechanical properties to load gravity loads. When there is a degenerative change in the intervertebral disc, the first step is a decrease in the water content and proteoglycan composition of the nucleus pulposus tissue, leading to a decrease in mechanical properties, which in turn causes the fibrous ring tissue to bear excessive gravitational loads. As a result, the external fibrous ring tears and ruptures, and the internal nucleus pulposus tissue protrudes outward, becoming the cause of nerve compression [4]. Overall, IDD is the initiating factor of LDH, and the two have different characteristics in terms of anatomical relationship and pathological features. The relevant basic research on the protrusion of nucleus pulposus tissue will help explore the pathogenesis of LDH and construct treatment strategies. Therefore, these studies require a reliable animal model to provide an experimental platform.

However, currently the most commonly used research on intervertebral disc related diseases is the model of inducing IDD by puncturing the caudal intervertebral disc of mice or rats [5, 6]. This model only causes degenerative changes in the intervertebral disc and does not simulate the pathological characteristics of the nucleus pulposus tissue breaking through the annulus fibrosus and entering the spinal canal, making it difficult to simulate the compression of the spinal cord or nerve roots. Depending on the degree of herniation of the nucleus pulposus, it can be divided into two types: bulging and herniation. Among them, intervertebral disc herniation is further divided into central herniation, paramedian herniation, and extremely paramedian herniation according to the direction of herniation [7]. These different types of herniation will lead to different symptoms, and their pathological characteristics and treatment methods will also vary. Therefore, the development of an animal model of LDH with accurate positioning and controllable degree can be controlled will help to study the disease in vivo.

In this study, we constructed a rat model of lumbar disc herniation induced by puncture. Different lengths of puncture needles and puncture angles were used to prepare lumbar disc herniation of different degrees and types. Behavioral, imaging, and histological studies confirmed that this model conforms to the characteristics of lumbar disc herniation.

Methods

Animals

This study was approved by the Ethics Committee of the First Affiliated Hospital of the Army Medical University (AMUWEC20232941), and the sprague-dawley (SD) rats used were purchased from Jiangsu Huachuang Xinnuo Pharmaceutical Technology Co., Ltd (Jiangsu, China). Rats were housed at 22 ~ 25 ℃ with a cycle of 12 h light and 12 h dark and free access to a pelleted commercial diet and water.

Design of intervertebral disc puncture needle

First, we used a micro computed tomography (Micro-CT) scanner (Skyscan1272, Bruker, Kontich, Belgium) to obtain the anatomical parameters of the rat L5/6 intervertebral disc. Specifically, male SD rats weighing about 300 ~ 400 g were selected and dissected after CO2 asphyxiation and euthanasia to obtain lumbar spine specimens for scanning. Image acquisition was performed at 60 kV and 165 μA with a resolution of 5 μm per voxel and acquisition time of 350 ms. 2D images were reconstructed using NRecon software v1.7.4.2 (Bruker, Kontich, Belgium). 3D images were reconstructed using CTvox software v3.3.1 (Bruker, Kontich, Belgium).Then the length of the puncture needle is determined according to the diameter of the intervertebral disc, and the outer diameter of the puncture needle is determined according to the height of the intervertebral disc, so as to ensure that the puncture needle can penetrate the anterior and posterior fibrous annulus of the rat L5/6 intervertebral disc, and just enter the spinal canal without damaging the spinal cord and nerves. In addition, select a needle of the same length according to the inner diameter of the puncture needle, which can be inserted into the puncture needle to push out the nucleus pulposus tissue inside the puncture needle.

Surgical procedures

Preoperative Preparation

The rats were used for model construction after one week of adaptive feeding, and all rats used for surgery were in good health before surgery. All rats were stopped from eating for 8 h before surgery.

Anesthesia method

Anesthesia was induced using isoflurane gas. Specifically, anesthesia induction was initiated by setting the oxygen flow rate to 2 L/min and adjusting the isoflurane

concentration to 5%. The induction chamber was pre-oxygenated for 1 min before placing rats inside. Close observation of behavioral changes was maintained, and animals were removed from the chamber when palpebral reflexes diminished. For anesthesia maintenance, a facemask inhalation technique was employed with the anesthesia machine set to maintain isoflurane concentration at 2~3% and oxygen flow rate at 1 L/min. Vital signs including heart rate and respiratory rate were continuously monitored during anesthesia, with adjustments made to isoflurane concentration and oxygen flow rate as needed based on anesthesia depth assessment. During the recovery phase, isoflurane administration was discontinued 5 min prior to the conclusion of the procedure. Oxygen inhalation was maintained until spontaneous respiration resumed, at which point animals were transferred to a thermostatically controlled recovery chamber (37 °C).

Surgical steps

All rats were randomly assigned to either the control group or experimental group. Under general anesthesia, animals were placed in a left lateral recumbent position on the operating table. The right lumbar region was depilated, disinfected with iodine solution, and a 2 cm incision was made from the iliac crest to the subcostal area. Sequential incision through skin, subcutaneous tissue, and abdominal wall muscles provided peritoneal access, exposing retroperitoneal adipose tissue. During the incision of the abdominal wall, pay attention to lifting the abdominal musculature to avoid damage to the abdominal organs. Blunt dissection of retroperitoneal fat revealed the ascending lumbar vein, which was used as a landmark for identifying the L5/6 intervertebral disc. Subsequent blunt separation between the psoas major and erector spinae muscles accessed the anterior vertebral column, exposing the L5/6 disc space. This approach avoided injury to major vessels including the inferior vena cava anterior to the vertebral body, but it should be noted that excessive separation of the upper and lower vertebrae should not be done to avoid damage to the anterior nourishing veins of the vertebrae. In the control group, the procedure concluded at this stage with layered closure. For the experimental group, a 22G blunt needle was advanced into the L5/6 disc after initial puncture of the anterior annulus fibrosus with a sharp needle to facilitate access. A 28G blunt needle was then inserted through the 22G cannula to extrude nuclear pulposus tissue. Surgical schematics and critical steps are illustrated in Fig. 1.

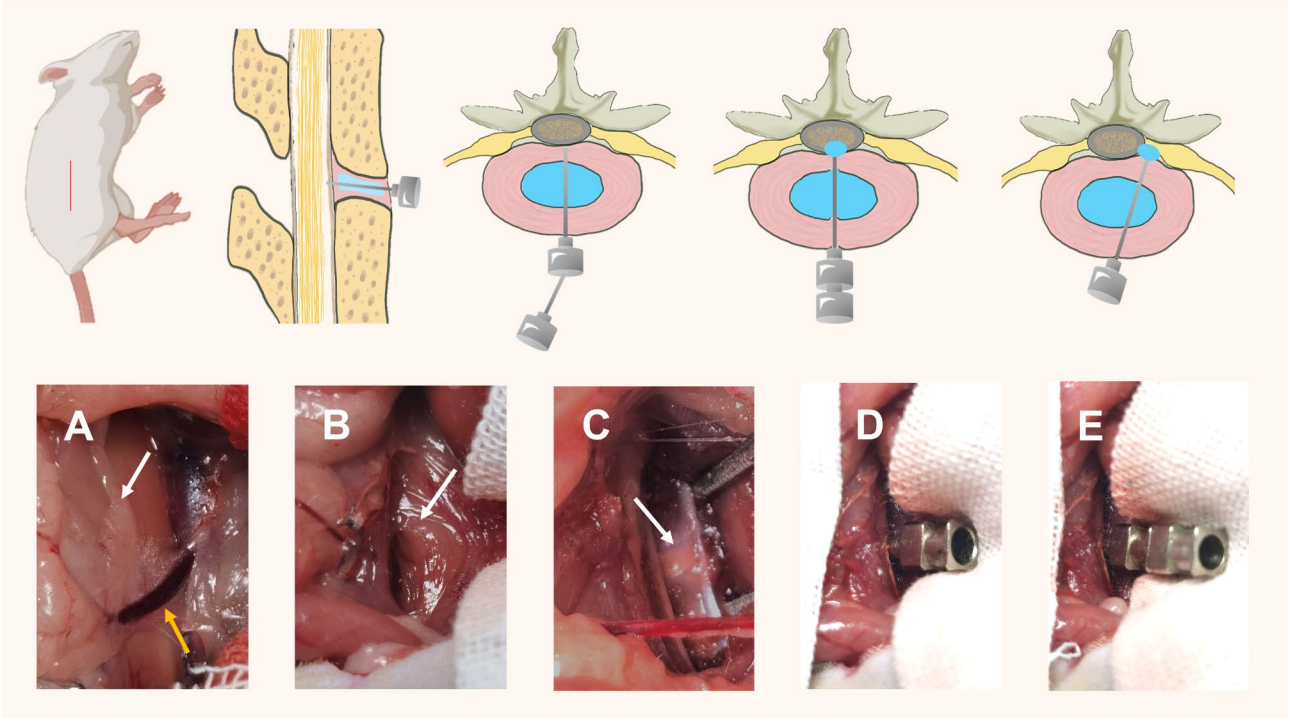

Fig. 1 Schematic diagram and surgical steps for constructing LDH rat model. (**A**) Blunt separation of retroperitoneal fat tissue, with white arrows indicating adipose tissue and yellow arrows indicating reflux veins; (**B**) Bluntly separating the erector spine and lumbar muscles, with white arrows indicating muscle gaps; (**C**) Expose L5/L6 intervertebral discs, with white arrows indicating the intervertebral discs; (**D**) Puncture of intervertebral disc; (**E**) Push the nucleus pulposus tissue backwards

Postoperative management

Post-procedure, rats were monitored for anesthetic recovery. Upon complete arousal, animals were transferred to individual housing cages and allowed ad libitum access to food and water for 4 h post-procedure. Surgical incisions were inspected daily, and cleaned with iodophor if bleeding or discharge was observed.

Construction strategy of intervertebral disc protrusion model

In the process of puncturing intervertebral discs, we can use different lengths of puncture needles and different puncture angles to construct models of different types of lumbar disc herniation. Therefore, the experimental group is further divided into degeneration group, bulging group, central herniation group, and paramedian herniation group. Specifically, based on the previously measured L5/6 intervertebral disc parameters in rats (Table. S1), a 3 mm long puncture needle was used to puncture only into the nucleus pulposus tissue without damaging the posterior fibrous ring; A 4 mm needle can push the nucleus pulposus tissue towards the back of the vertebral body; A 5 mm needle can puncture the posterior fibrous ring. In terms of puncture angle, when the puncture needle is parallel to the sagittal direction, it can push the nucleus pulposus tissue towards the center position; A 20° angle with the sagittal direction can push the nucleus pulposus tissue towards the intervertebral foramen position.

Ethology evaluation

The Von Frey tests were performed 1 day, 3 days, 5 days, 1 week, 2 weeks, and 3 weeks postoperatively to assess the mechanical pain threshold of rats. Before conducting testing, first place rats separately in a dedicated cage and let them rest for 20 min. After the rats have calmed down, a Von Frey hairs pain tester (NC12775-99, North Coast, USA) was used for testing (Fig. S3), start with the finer fibers and use appropriate force that can bend the fibers to stimulate the soles of the hind feet of the rats. Repeat the stimulation for 5 times. If the rats experience retraction or licking of the hind feet in 3 of these times, it is recorded as positive. Otherwise, continue to use thicker fibers for testing. In addition, at the same time point after surgery, the exercise ability of the rats was evaluated using the Basso, Beattie, Bresnahan locomotor rating scale (BBB scale, Table. S2) [8].

Imaging evaluation

On the one week after surgery, the lumbar intervertebral discs of rats were observed using a magnetic resonance imaging (MRI) scanner (7.0 Tesla MRI system, Bruker Pharmascan). T2-weighted sagittal and axial images were collected in 11 consecutive slices (thickness 0.8 mm), the field of view was 40 × 40 mm, and the matrix size was 256 × 256 (Echo time = 35ms, Echo spacing = 11.667ms, Repetition time = 3000ms, 1 Repetitions, 2 Averages, Scan time = 6min24s). Bee DICOM Viewer v3.7.1 (Sino Union, Beijing, China) was used to observe images.

Histological staining

One week after surgery, a specimen of the lumbar vertebrae from 5 to 6 segments was obtained after euthanasia in rats. After 48 h of fixation with 4% paraformaldehyde, it was decalcified with 10% EDTA for one month, then dehydrated and embedded with optimal cutting temperature (OCT) compound. The specimen was frozen sectioned parallel to the axis, with a thickness of 10 μm. Immediately, the tissue slices were stained with hematoxylin-eosin (H&E) and safranin-O/fast green (SF) staining. In addition, we also quantitatively analyzed different types of intervertebral discs according to the histological scoring method of intervertebral discs (Table. S3) [9].

Immunofluorescence staining

Place the prepared tissue slices at room temperature for 30 min, Soak PBS for 10 min to wash off OCT. Then, incubate with 0.5% Triton X-100 at room temperature for 10 min and 5% BSA blocking solution for 1 h. Subsequently, the slices were combined with first antibody (anti-ACAN, 1:200; anti-IL-1β, 1:200; anti-TNF-α, 1:200; anti-CD31;1:200) incubate overnight at 4 ℃. Then incubate with secondary antibody at room temperature for 1 h, and finally stain and seal with DAPI. Immuno-histochemical sections were scanned on full glass slides, while immunofluorescence sections were detected using confocal laser scanning microscopy (CLSM) (ZISS 880, ZISS, Germany). Finally, use Image J software to calculate the staining area, cell count, and average fluorescence density.

Statistical analysis

Perform statistical analysis using GraphPad Prism v9.5.1 (GraphPad, Boston, USA). Quantitative data are expressed as mean ± standard deviation, and independent sample t-tests are used for inter group comparisons. $P < 0.05$ indicates a statistically significant difference.

Results

IVD parameters

We measured the anterior and posterior diameters and heights of L5/6 intervertebral discs in rats weighing around 300~400 g. As shown in Fig. 2, select the midpoint of the line connecting the anterior and posterior edges of the L5 vertebral body to measure the diameter of the intervertebral disc, and select the line connecting the midpoint of the lower edge of the L5 vertebral body to the midpoint of the upper edge of the L6 vertebral

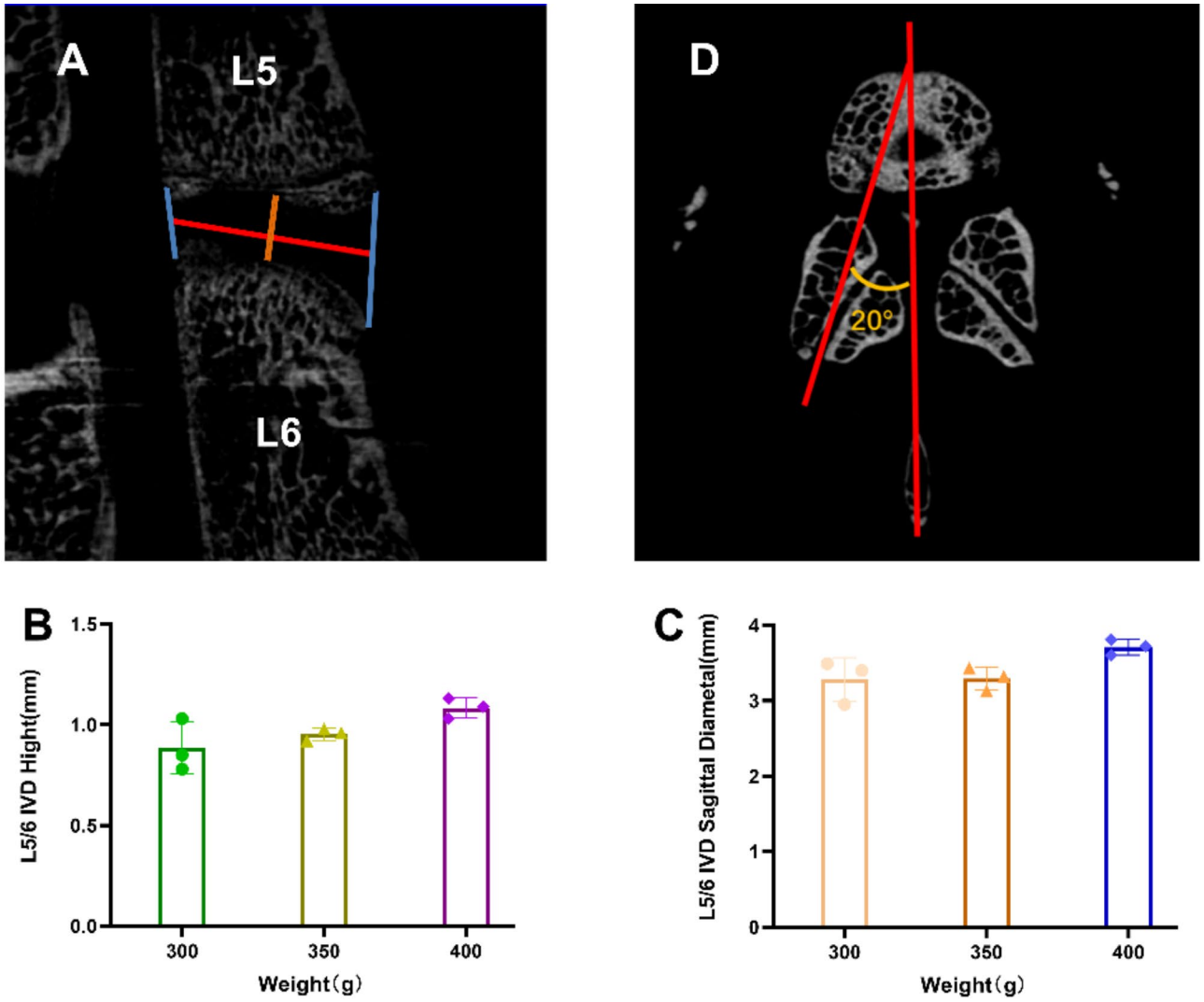

Fig. 2 Parameters of L5/L6 intervertebral discs in rats. (**A**) Schematic diagram of disc diameter and height measurement; (**B**) L5/L6 intervertebral disc diameter in rats of different body weights; (**C**) The average height of L5/L6 intervertebral discs in rats of different weights; (**D**) Schematic diagram of intervertebral foramen angle measurement

body to measure the height of the intervertebral disc. The average diameter and height of L5/6 intervertebral discs in rats weighing around 300 g, 350 g, and 400 g were 3.28 mm, 3.29 mm, and 3.71 mm, respectively. Their intervertebral disc heights were 0.89 mm, 0.95 mm, and 1.08 mm, respectively (Fig. 2). Based on this parameter, we have determined the specifications of the puncture needle. A 22G blunt needle with an outer diameter of 0.71 mm and an inner diameter of 0.41 mm was selected as the needle for puncturing intervertebral discs. A 28G needle with an outer diameter of 0.35 mm was inserted into the 22G puncture needle.

In addition, we also measured the angle of the intervertebral foramen, as shown in Fig. 2D, which is about 20 °. Therefore, during the puncture, when the puncture is parallel to the sagittal line, the nucleus pulposus tissue can be pushed towards the center of the spinal canal; when the puncture angle is at an angle of 20° to the sagittal line, the nucleus pulposus tissue can be pushed towards the position of the intervertebral foramen.

Imaging evaluation

We performed MRI on rats from different groups in the experimental group one week after surgery (Fig. 3). MRI T2 sagittal images show that compared to other segments of intervertebral discs, the signal of L5/6 intervertebral discs is reduced, indicating degenerative changes. The 3 mm puncture needle only caused intervertebral disc degeneration, while the 5 mm puncture needle can cause intervertebral disc protrusion into the spinal canal. MRI T2 axial images show that different puncture angles can cause different types of intervertebral disc herniation.

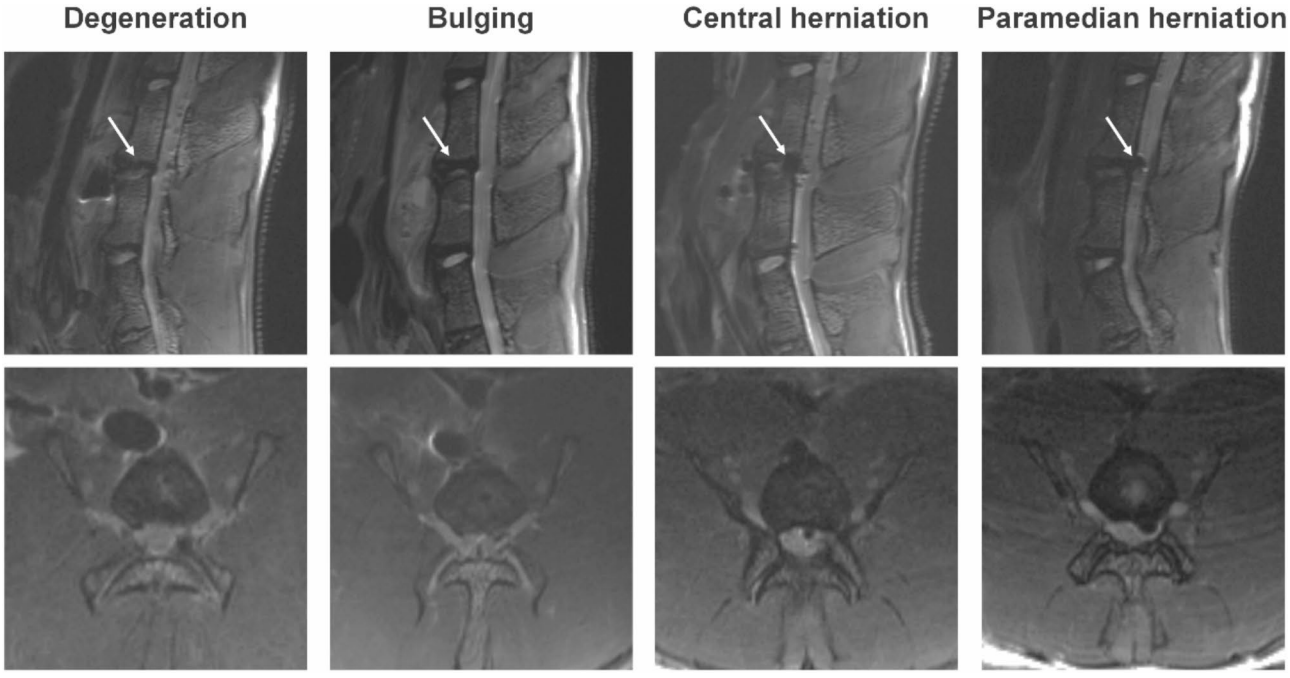

Fig. 3 LDH model rat 7T MRI T2 sagittal and axial images. The signal of the L5/6 intervertebral disc in the degenerative group decreased, while the nucleus pulposus tissue in the bulging group protruded backwards without entering the spinal canal. The nucleus pulposus tissue of the central herniation group and the paramedian herniation group protruded into the spinal canal and intervertebral foramen, respectively. White arrows indicate degenerated or herniated L5/6 discs

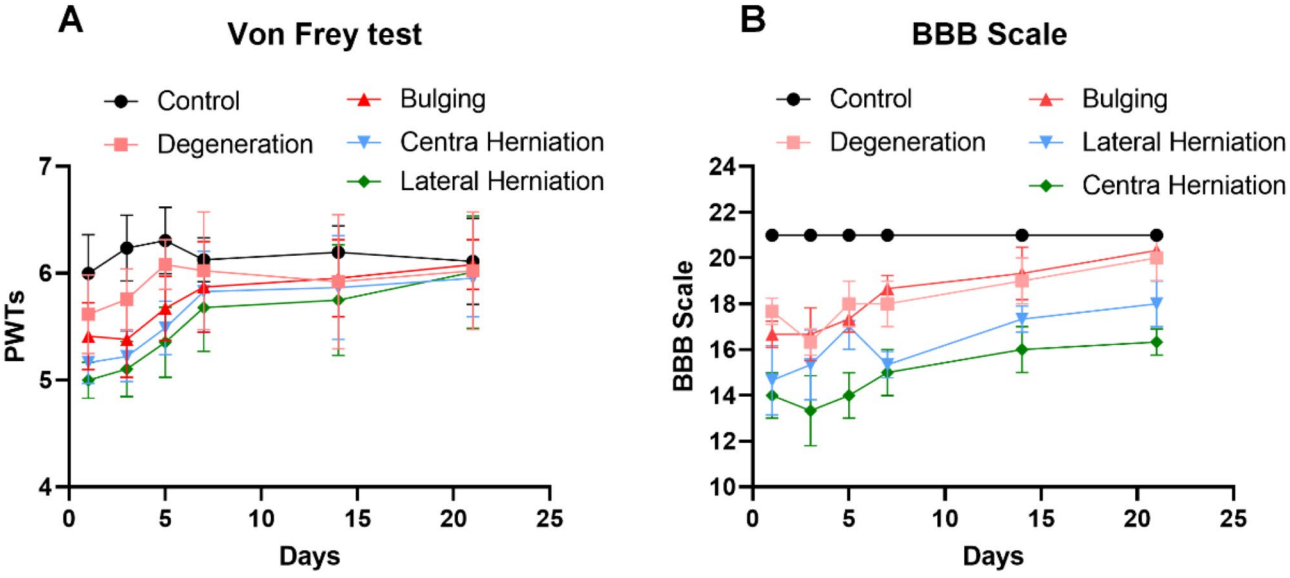

Fig. 4 Ethology evaluation of LDH rats. (**A**) Von Frey test; (**B**) BBB scale

When the puncture angle is parallel to the sagittal direction, it can cause central herniation, and when the puncture angle is at a 20° angle to the sagittal direction, it can cause paramedian herniation.

Ethology evaluation

Ethology evaluations of the rats at different time points after surgery suggest that the experimental group of rats exhibited varying degrees of neurological damage symptoms. As shown in Fig. 4A, in the Von Frey test, the Paw Withdrawal Thresholds (PWTs) values of normal rats in the control group were stable at around 6, with small fluctuations, indicating no significant change in pain sensitivity. However, the initial PWTs values of the degenerative and bulging groups were lower but higher than those of the central and paracentric bulge groups. Over

time, the degenerative group recovered rapidly to the normal group, and the bulging and two bulges also recovered slowly. Eventually, the pain sensitivity of all degenerative and bulging groups returned to normal levels. The specific statistics are shown in Table. S4.

As shown in Fig. 4B, the BBB score results showed similar results to those of the Von Frey test. In the early stage after model construction, both degenerative and prominent model rats showed varying degrees of motor function impairment. Subsequently, the motor function of the degenerative and bulging groups gradually returned to normal, and the motor function recovery of the central and paracentric herniation groups was significantly lower than that of the other groups, indicating that the protruding nucleus pulposus tissue continued to compress the spinal cord. The specific statistics are shown in Table. S5.

Histology evaluation

We conducted histological evaluation on LDH rats that were successfully modeled. As shown in Fig. 5A, H&E staining and SF staining indicate that compared with the intervertebral disc tissue of the normal group rats, intervertebral disc tissues of different protrusion types show typical pathological changes. The IDD group showed disorder of the fibrous ring, significant degeneration of the nucleus pulposus tissue, and decreased content of nucleus pulposus cells and extracellular matrix. In the bulging IVD group, the posterior fibrous ring is intact, the intervertebral disc nucleus pulposus tissue protrudes into the spinal canal, and the spinal cord is mildly compressed. The central protrusion group shows a rupture of the posterior fibrous ring, with the nucleus pulposus tissue entering the spinal canal and significant compression of the spinal cord. The lateral protrusion group shows that the nucleus pulposus tissue protrudes into the intervertebral foramen, and the nerve roots are compressed. The histological grade results are shown in Fig. 5B. Compared with the normal group, the histological grades of intervertebral discs in each experimental group were higher, and the grades in the two herniation groups were higher than those in the degeneration group and the bulging group.

Immunofluorescence staining of the aggrecan (ACAN) with the highest content in the nucleus pulposus tissue showed a significant decrease in proteoglycan content in intervertebral disc tissues of different protrusion types, while the expression of proteoglycans in protruding tissues increased, further confirming that the protruding tissue originates from the intervertebral disc and is consistent with the pathological changes of intervertebral disc herniation (Fig. 6).

Immunofluorescence staining of inflammatory factors showed that in the central part of the degenerated intervertebral disc and the herniated part of the both herniation disc, the expression of IL-1β and TNF-α in the nucleus pulposus was elevated (Fig. 7), indicating that the nucleus pulposus tissue was undergoing an inflammatory immune response.

After the protrusion of intervertebral disc tissue into the spinal canal, it is often accompanied by the generation of a large number of new blood vessels, which is a pathological change closely related to inflammation. We performed corresponding immunofluorescence staining on intervertebral disc tissues with different types of protrusions. As shown in Fig. 8, significant high expression of the vascular endothelial marker CD31 can be observed around the protruding intervertebral disc tissue, indicating a large amount of neovascularization in these tissues.

Discussion

Understanding the pathogenesis, pathological outcomes, and treatment methods of LDH cannot be separated from animal model research. Mammals have a similar intervertebral disc structure to humans and are often used in the construction of intervertebral disc related disease models. The anatomical structure and biomechanical characteristics of intervertebral discs in large animals such as pigs and goats are similar to those of humans, making them an ideal choice for constructing LDH models [10, 11]. However, their high economic cost and difficulty in operation limit their widespread application. Small animals such as rabbits and mice are currently the most commonly used animals for constructing intervertebral disc disease models [12, 13]. Among them, the tail vertebrae acupuncture IDD model of rats and mice is a classic method with advantages of simple operation, reliability, and high stability, making it the first choice for studying IDD [14]. However, there are structural differences between the coccyx and lumbar vertebrae. Although both have the same intervertebral disc structure, the difference in the morphology of the coccyx cone results in a lack of spinal canal structure and the absence of spinal cord and nerve roots. These characteristics make it difficult for the coccyx puncture model to simulate the compression of the posterior spinal cord or nerve roots after herniation, and it is also difficult to study the microenvironmental changes of intervertebral disc tissue such as the nucleus pulposus entering the canalis spinalis [15].

Previous studies have simulated the changes of the nucleus pulposus entering the spinal canal and breaking through the original blood and immune barriers by heterotopic transplantation of intervertebral disc tissue into the muscle gap [16]. Although this method can expose the nucleus pulposus tissue to the immune environment to a certain extent, it still cannot fully restore the biomechanical and pathophysiological characteristics of intervertebral disc herniation, especially the microenvironment inside the spinal canal is difficult to replicate.

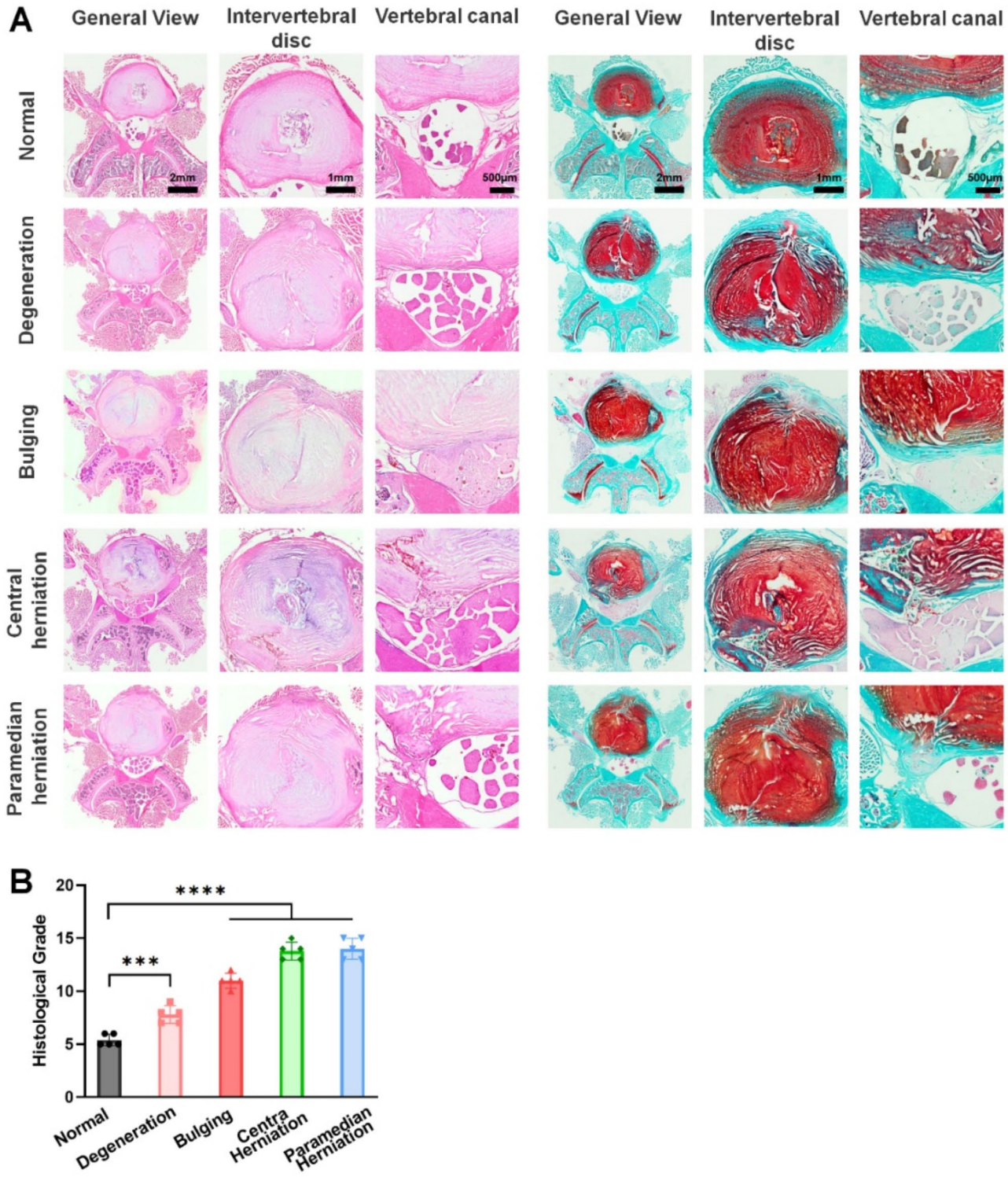

Fig. 5 H&E and SF images of intervertebral disc tissues with different types of herniation and histological grade. (**A**) Overall and magnified images of H&E and SF staining of the L5/6 intervertebral discs in rats from different groups. Magnified images are used to reveal details of structural changes in the disc and herniated nucleus pulposus. (**B**) Quantitative analysis of histological grade of L5/6 intervertebral disc in different groups of rats, ***<0.001, ****<0.0001

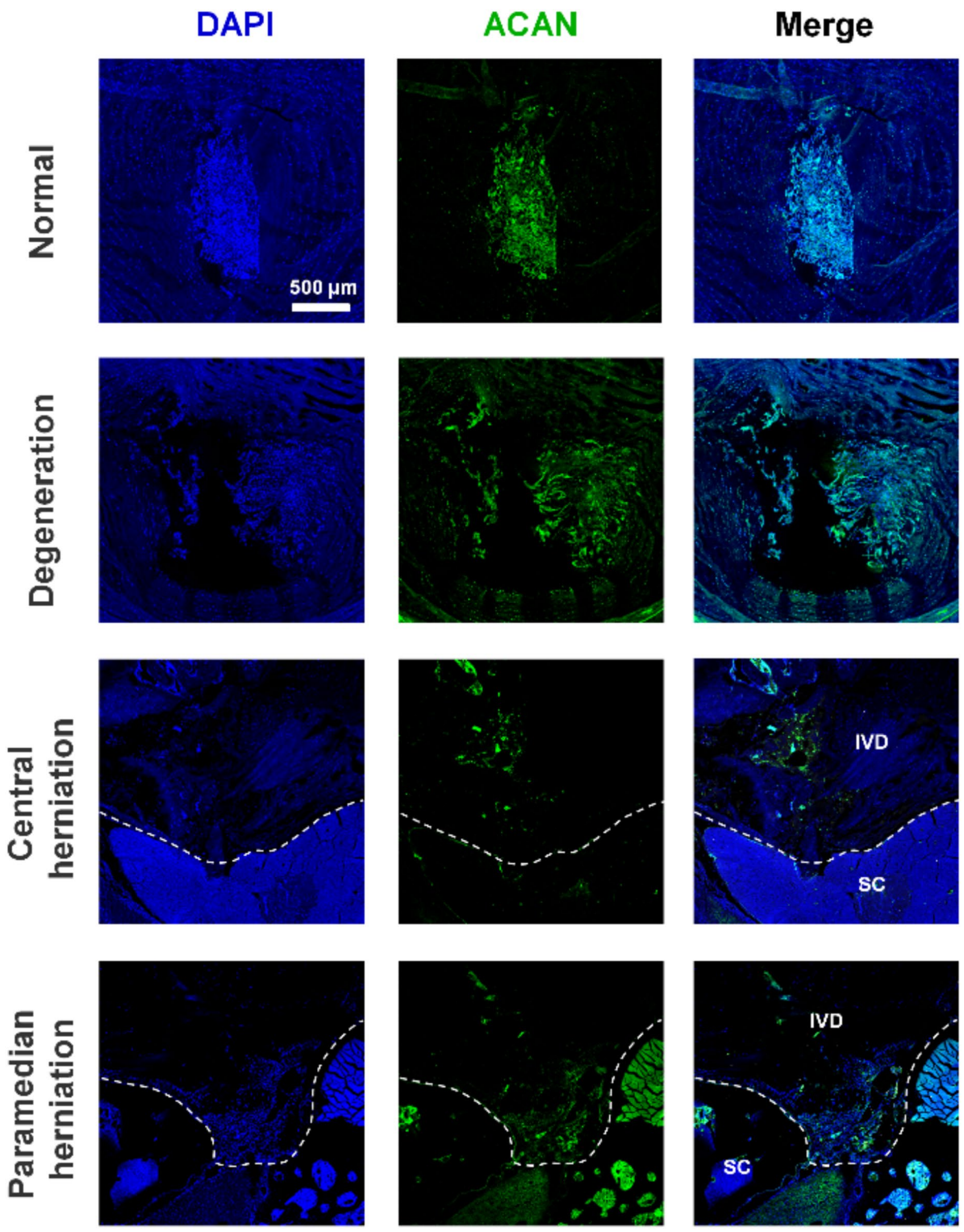

Fig. 6 Immunofluorescence images of ACAN of intervertebral disc tissues with different types of herniation. Blue fluorescence represents DAPI staining of nucleus, green fluorescence represents ACAN staining. In normal group, the nucleus pulposus was full and green fluorescence was aggregated; the degeneration intervertebral disc nucleus pulposus was destroyed and the fluorescence area was reduced; the central and paramedian herniation discs detected green fluorescence signals at the herniated site

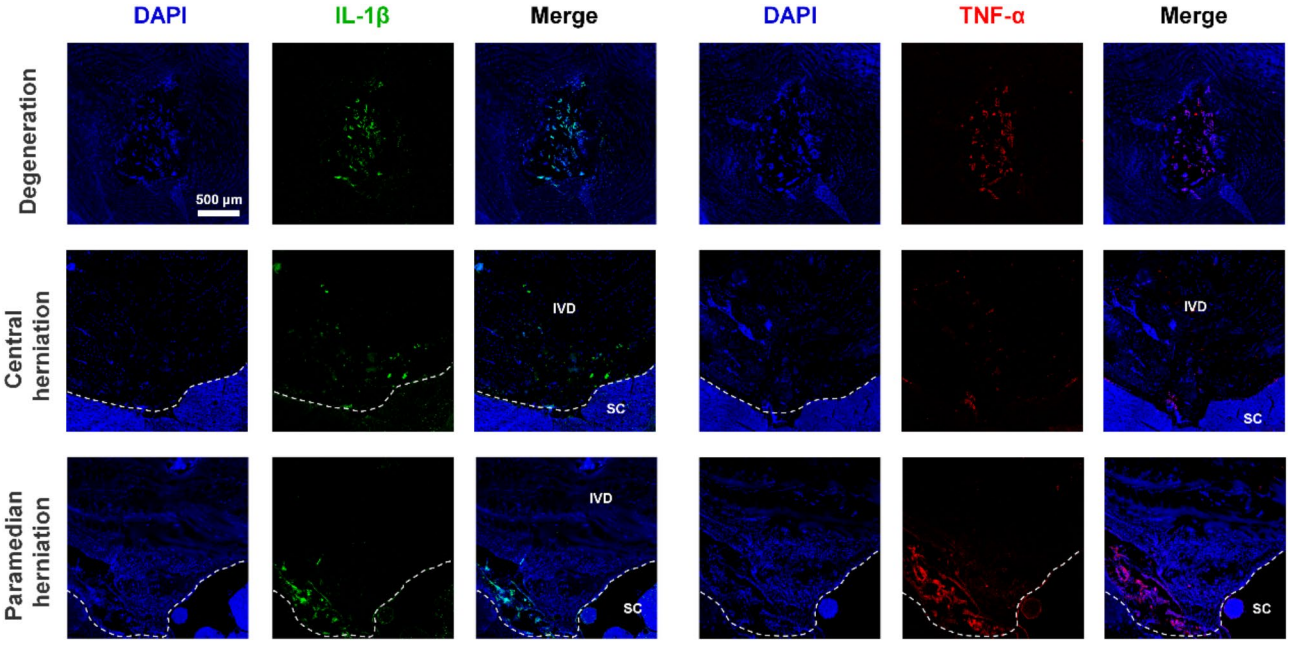

Fig. 7 Immunofluorescence images of IL-1β and TNF-α of intervertebral disc tissues with different types of herniation. Green fluorescence represents IL-1β staining, while red fluorescence represents TNF-α staining. High expression of both IL-1β and TNF-α was detected in the central nucleus pulposus of degenerated intervertebral discs and in the central and paramedian herniation disc herniated site

Therefore, some studies have simulated the stimulating effect of intervertebral disc tissue on nerves by transplanting autologous intervertebral discs from the rat tail vertebra to the L5 nerve root [17]. However, this surgical method requires the destruction of structures such as the vertebral plate and articular processes through a posterior approach to expose the nerve root, which can lead to changes in the biomechanical characteristics of the spine. In this study, we used a lateral approach to separate the space between the psoas major muscle and the erector spine muscle, exposing the intervertebral discs of the lumbar 5/6 segment. The intervertebral discs were directly punctured and the nucleus pulposus tissue was pushed into the spinal canal to cause disc herniation, minimizing trauma and preserving the anatomical structure of the spine, which is similar to the anatomical and pathological characteristics of human lumbar disc herniation. In addition, the stimulation of the protruding nucleus pulposus tissue on the spinal cord or nerve root can lead to corresponding sensory and motor dysfunction. In the LDH model we constructed, rats in different groups experienced varying degrees of sensory and motor dysfunction after surgery, and this obstacle gradually recovered over time, indicating that we have successfully simulated the behavioral characteristics of lumbar disc herniation, which is something that has been less studied in animal models of intervertebral disc disease in the past.

Unlike most previous animal studies on intervertebral discs that used sagittal or coronal tissue sections, we performed axial tissue sections on the obtained rat spinal specimens. This sectioning method not only preserves the fibrous ring and nucleus pulposus tissue to the greatest extent possible, but also allows for a more complete observation of the complete anatomical structure of the spine, such as the spinal canal, spinal cord, nerve root, and intervertebral foramen. This helps us study the relationship between nucleus pulposus tissue protrusion and adjacent tissue structures, such as nerve roots and spinal cord. As shown in Fig. 5, in the different types of intervertebral disc degeneration or protrusion models we constructed, the structure of the intervertebral disc, such as the annulus fibrosus and nucleus pulposus, showed varying degrees of pathological changes, which also conform to the characteristics of human intervertebral disc degeneration and protrusion. In detail, the degeneration of intervertebral disc nucleus pulposus tissue results in water loss, decreased nucleus pulposus cells, and decreased proteoglycan content [18]. As the degree of degeneration worsens, the height of the intervertebral space will decrease, further causing the nucleus pulposus tissue to protrude backwards until the annulus fibrosus ruptures and eventually protrudes. This process will lead to a progressive decrease in nucleus pulposus cells and proteoglycans [19]. In our study, H&E and safranin green staining confirmed this pathological process.

A mature intervertebral disc is a tissue lacking blood supply, and the nutritional supply and metabolic exchange within the disc mainly rely on the upper and lower endplates and fibrous rings to penetrate into the

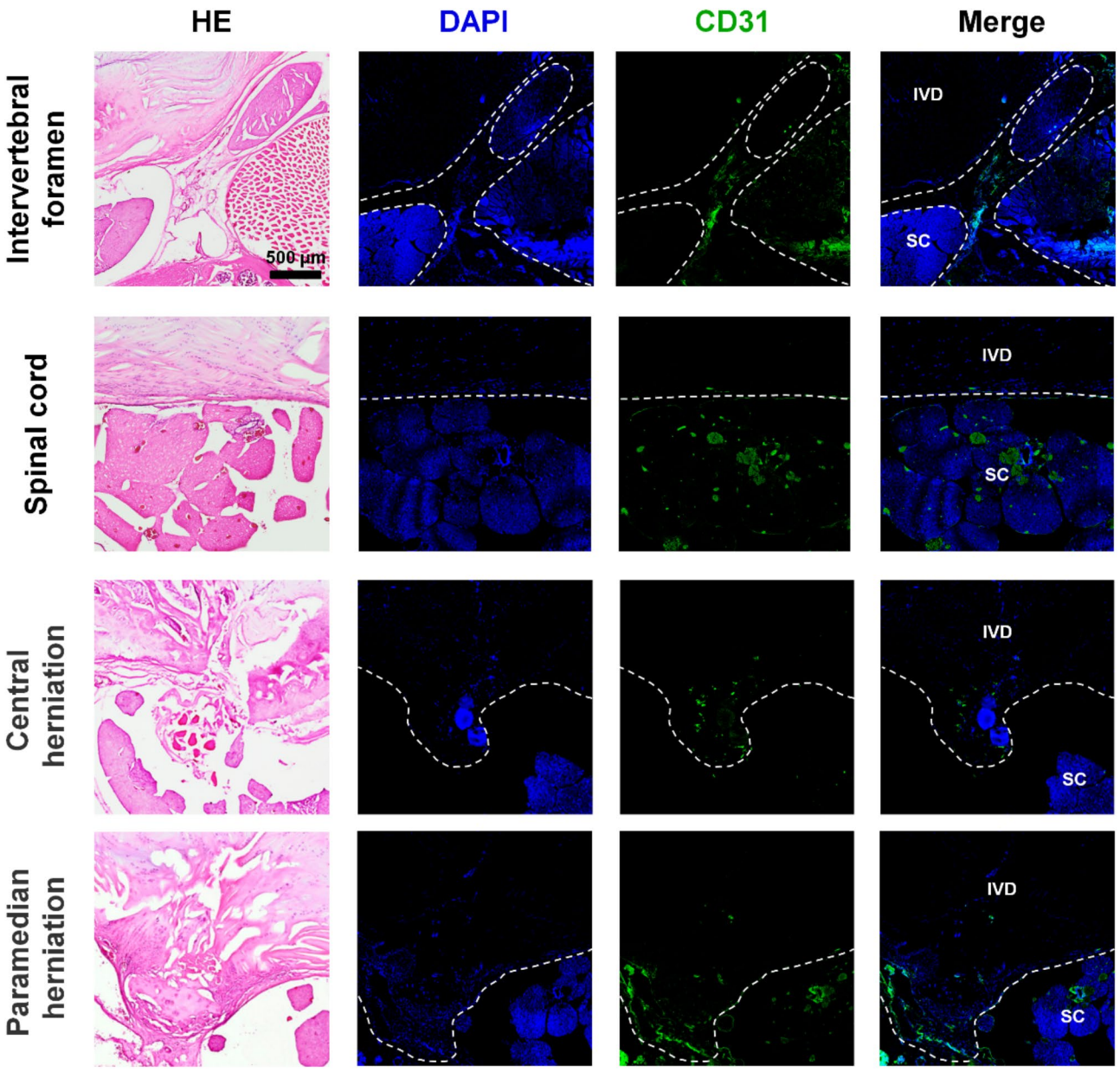

Fig. 8 Immunofluorescence images of CD31 of intervertebral disc tissues with different types of herniation. In H&E images, there are a large number of red blood cells around the intervertebral foramen, spinal cord, and herniated intervertebral disc tissue. In the immunofluorescence image, it can be seen that these areas highly express CD31

nucleus pulposus tissue [20]. As shown in Fig. 8, there is abundant blood supply in the intervertebral foramen and spinal cord, and a large number of red blood cells can be seen in HE staining. Red blood cells are also found to penetrate into the center of the intervertebral disc at the damaged annulus fibrosus. Further immunofluorescence revealed the presence of numerous vascular structures in the intervertebral foramen, dural sac, and spinal cord, indicating that when the fibrous ring ruptures and the nucleus pulposus tissue protrudes, it can enter the spinal canal and come into contact with the dural sac or enter the intervertebral foramen, providing a basis for the occurrence of inflammatory reactions and the generation of new blood vessels. In addition, some scholars believe that the growth of new blood vessels is the cause of annulus fibrosus tear [21]. In any case, the model we built can provide a basis for subsequent research on the relationship between disc herniation and blood supply.

This study has several limitations. Firstly, exposing the lumbar intervertebral disc through the interspace between the psoas major and erector spine muscles requires familiarity with the corresponding anatomical

structure and a certain level of surgical proficiency, as well as a certain learning curve. Secondly, puncturing the intervertebral disc in front of the spine can cause rupture of the anterior fibrous ring, which is not consistent with the specific condition of intervertebral disc herniation in humans. In addition, rats are non-upright walking animals, and there are certain differences in the biomechanical characteristics of the lumbar vertebrae compared to humans. The pressure load on the intervertebral discs is relatively small, and it will not bring sustained pressure to the protruding intervertebral disc tissue. This may be one of the reasons why LDH rats recover from sensory and motor disorders quickly. Finally, we only analyzed the histopathological changes at one time point and did not continuously observe the pathological characteristics of rat intervertebral disc herniation over a period of time. In the future, more time points are needed to analyze the characteristics of intervertebral disc tissue herniation at different stages.

Conclusions

In conclusion, we have innovatively constructed a precise localization and degree-controllable rat model of LDH, which can simulate different types of LDH. This rat model can provide a stable and reliable experimental platform with low time and economic cost for in vivo research on the pathogenesis, pathological changes, and treatment methods of LDH.

Abbreviations

LDH	Lumbar disc herniation
IDD	Intervertebral disc degeneration
SD rats	Sprague-dawley rats
Micro-CT	Micro Computed tomography
BBB scale	Basso, Beattie, Bresnahan scale
MRI	Magnetic resonance imaging
H&E	Hematoxylin-eosin
SF	Safranin-O/fast green
CLSM	Confocal laser scanning microscopy
ACAN	Aggrecan

Supplementary Information

The online version contains supplementary material available at https://doi.org/10.1186/s13018-025-05710-6.

Supplementary Material 1

Acknowledgements

Not applicable.

Author contributions

MY and JLZ performed all experiments and data analysis and drafted the manuscript. QDY, BY and JC provided administrative, technical or material support, and interpreted the results. TYH designed and supervised the study and edited the manuscript. All authors read and approved the final manuscript.

Funding

The study was supported by the Science and Health Joint Project of Chongqing (2022ZDXM010), Chongqing Young and Middle-aged Medical High-end Talent Project (YXGD202401) and the Major Project of Science and Technology Research Program of Chongqing Municipal Education Commission (KJZD-M202412801).

Data availability

Data is provided within the manuscript or supplementary information files.

Declarations

Ethics approval and consent to participate

This study was approved by the Ethics Committee of the First Affiliated Hospital of the Army Medical University (AMUWEC20232941).

Consent for publication

Not applicable.

Competing interests

The authors declare no competing interests.

Received: 6 February 2025 / Accepted: 12 March 2025
Published online: 25 March 2025

References

1. Zhang AS, Xu A, Ansari K, et al. Lumbar disc herniation: diagnosis and management. Am J Med. 2023;136(7):645–51.
2. Knezevic NN, Candido KD, Vlaeyen JWS, Van Zundert J, Cohen SP. Low back pain. Lancet (London England). 2021;398(10294):78–92.
3. Song Z, Yan M, Zhang S, et al. Implications of circadian disruption on intervertebral disc degeneration: the mediating role of sympathetic nervous system. Ageing Res Rev. 2024;104:102633.
4. Wang F, Cai F, Shi R, Wang XH, Wu XT. Aging and age related stresses: a senescence mechanism of intervertebral disc degeneration. Osteoarthr Cartil. 2016;24(3):398–408.
5. Hong JY, Kim H, Jeon WJ, et al. Animal models of intervertebral disc diseases: advantages, limitations, and future directions. Neurol Int. 2024;16(6):1788–818.
6. Wang Y, Kang J, Guo X, et al. Intervertebral disc degeneration models for pathophysiology and regenerative therapy -Benefits and limitations. J Invest Surgery: Official J Acad Surg Res. 2022;35(4):935–52.
7. Hornung AL, Barajas JN, Rudisill SS, et al. Prediction of lumbar disc herniation resorption in symptomatic patients: a prospective, multi-imaging and clinical phenotype study. Spine Journal: Official J North Am Spine Soc. 2023;23(2):247–60.
8. Basso DM, Beattie MS, Bresnahan JC. A sensitive and reliable locomotor rating scale for open field testing in rats. J Neurotrauma. 1995;12(1):1–21.
9. Mao HJ, Chen QX, Han B, et al. The effect of injection volume on disc degeneration in a rat tail model. Spine. 2011;36(16):E1062–9.
10. Zhang C, Gullbrand SE, Schaer TP, et al. Inflammatory cytokine and catabolic enzyme expression in a goat model of intervertebral disc degeneration. J Orthop Research: Official Publication Orthop Res Soc. 2020;38(11):2521–31.
11. Gullbrand SE, Malhotra NR, Schaer TP, et al. A large animal model that recapitulates the spectrum of human intervertebral disc degeneration. Osteoarthr Cartil. 2017;25(1):146–56.
12. Calvo-Echenique A, Cegoñino J, Correa-Martín L, Bances L, Palomar AP. Intervertebral disc degeneration: an experimental and numerical study using a rabbit model. Med Biol Eng Comput. 2018;56(5):865–77.
13. Yao T, Gao J, You C, et al. A new animal model of lumbar disc degeneration in rabbits. Spine Journal: Official J North Am Spine Soc. 2024;24(8):1519–26.
14. Elmounedi N, Bahloul W, Aoui M, Sahnoun N, Ellouz Z, Keskes H. Original animal model of lumbar disc degeneration. Libyan J Med. 2023;18(1):2212481.
15. Daly C, Ghosh P, Jenkin G, Oehme D, Goldschlager T. A review of animal models of intervertebral disc degeneration: pathophysiology, regeneration, and translation to the clinic. Biomed Res Int. 2016;2016:5952165.
16. Lu X, Chen L, Jiang C, Cao K, Gao Z, Wang Y. Microglia and macrophages contribute to the development and maintenance of sciatica in lumbar disc herniation. Pain. 2023;164(2):362–74.
17. Kim SJ, Park SM, Cho YW, et al. Changes in expression of mRNA for interleukin-8 and effects of interleukin-8 receptor inhibitor in the spinal dorsal Horn in a rat model of lumbar disc herniation. Spine. 2011;36(25):2139–46.

18. Kang L, Zhang H, Jia C, Zhang R, Shen C. Epigenetic modifications of inflammation in intervertebral disc degeneration. Ageing Res Rev. 2023;87:101902.
19. Mohd Isa IL, Teoh SL, Mohd Nor NH, Mokhtar SA. Discogenic low back pain: anatomy, pathophysiology and treatments of intervertebral disc degeneration. Int J Mol Sci. 2022;24(1).
20. Francisco V, Ait Eldjoudi D, González-Rodríguez M, et al. Metabolomic signature and molecular profile of normal and degenerated human intervertebral disc cells. Spine Journal: Official J North Am Spine Soc. 2023;23(10):1549–62.
21. Peredo AP, Gullbrand SE, Mauck RL, Smith HE. A challenging playing field: identifying the endogenous impediments to annulus fibrosus repair. JOR Spine. 2021;4(1):e1133.

Publisher's note